Available online at www.sciencedirect.com
SCIENCE DIRECT
Tetrahedron 62 (2006) 4232–4242
Tetrahedron

Reactivity and regioselectivity in the synthesis of spiroindoles via indole *o*-quinodimethanes. An experimental and computational study

Constantinos A. Tsoleridis,* John Dimtsas, Dimitra Hatzimimikou and Julia Stephanidou-Stephanatou

Laboratory of Organic Chemistry, Department of Chemistry, University of Thessaloniki, 54124 Macedonia, Greece

Received 8 September 2005; revised 28 December 2005; accepted 19 January 2006

Available online 10 March 2006

Abstract—The 1,3-dipolar cycloaddition reactions of stable nitrile oxides with indole *o*-quinodimethanes have been examined. In all cases the '*exo–anti*' addition products, dispiroisoxazolines, were isolated in moderate to good yields (25–47%). In addition, from the reaction of one of the indole quinodimethanes with mesitonitrile oxide the '*exo–syn*' addition product was isolated in 7% yield along with the remarkable indole quinodimethane dimerization and cycloaddition product, which was isolated in 13% yield. An analogous dimerization and cycloaddition product was isolated in 18% yield from the reaction of the *N*-acetyl-indole quinodimethane with mesitonitrile oxide. In the case of the reaction of the *N*-benzoylindole quinodimethane with the 2,6-dichlorobenzonitrile oxide an oxime was also isolated in 13% yield. The proposed reaction mechanism is supported by semiempirical (AM1) MO calculations via FMO interactions. The observed selectivity was explained by an investigation of the transition states carried out also for analogous dispiroisoxazolines.
© 2006 Elsevier Ltd. All rights reserved.

1. Introduction

The chemistry of heterocyclic *o*-quinodimethanes (*o*-QDMs) has gained increasing interest in the last decade.[1] *o*-QDMs have been widely used as intermediates[2] in the synthesis of lignans,[3] terpenes, anthracyclines, alkaloids,[4] steroids and other natural products.[5–7] The study of their reactivity, applied in organic synthesis, is still an important issue.[1] However, although the utilization of *o*-QDM/Diels–Alder methodology in the synthesis of complex polycyclic compounds and the factors controlling the stereochemistry of the reaction have been studied extensively,[1,8] the 1,3-dipolar nitrile oxide cycloaddition to *o*-QDMs and moreover the 1,3-dipolar cycloaddition reactions with 1,3-dienes are rare.[9] To our knowledge, the only example of 1,3-dipolar cycloaddition to *o*-QDMs leading to spiro derivatives has been reported by us.[10]

Against this background, we have explored the reactivity of the stable nitrile oxides mesitonitrile oxide and 2,6-dichlorobenzonitrile oxide towards indole *o*-quinodimethanes speculating the formation of new spiroindoles, since spiroindole derivatives show interesting biological activities.[11–13] Our results revealing the facile formation of novel spiroindoles are presented here along with a reactivity and regioselectivity investigation of the reaction.

2. Results and discussion

The *N*-substituted 2,3-bis(bromomethyl)indoles **2** were synthesized by known procedures.[14,15] From these bisbromides **2** by treatment with sodium iodide in DMF at 150 °C the corresponding indole quinodimethanes **3** were generated in situ and were trapped with 2 mol equiv of nitrile oxide to afford moderate to good yields (31–47%) of products, by addition to the two exomethylenic double bonds (Scheme 1). In all cases the '*exo–anti*' dispiroindoles **5** were isolated (20–46% yield). It is of interest to note that from the reaction of the indole *o*-quinodimethane **3a** with mesitonitrile oxide the '*exo–syn*' dispiroindole **6a** was also isolated (7% yield) along with a third product, the dispiroindole compound **7a** in 13% yield. This very interesting product is most probably produced by 1,3-dipolar cycloaddition of a mesitonitrile oxide molecule to the exomethylene double bond $C_2{=}CH_2$ followed by the [4+2] cycloaddition of *o*-QDM to the remaining exomethylene double bond (see Section 2.2). An analogous product **7b** was isolated in 18% yield from the reaction of QDM **3b** with **4a**.

Keywords: Spiroindoles; *o*-Quinodimethanes; Diels–Alder reactions; Reactivity; Regioselectivity.
* Corresponding author. Tel.: +30 2310 997865; fax: +30 2310 997679; e-mail: tsolerid@chem.auth.gr

0040–4020/$ - see front matter © 2006 Elsevier Ltd. All rights reserved.
doi:10.1016/j.tet.2006.01.064

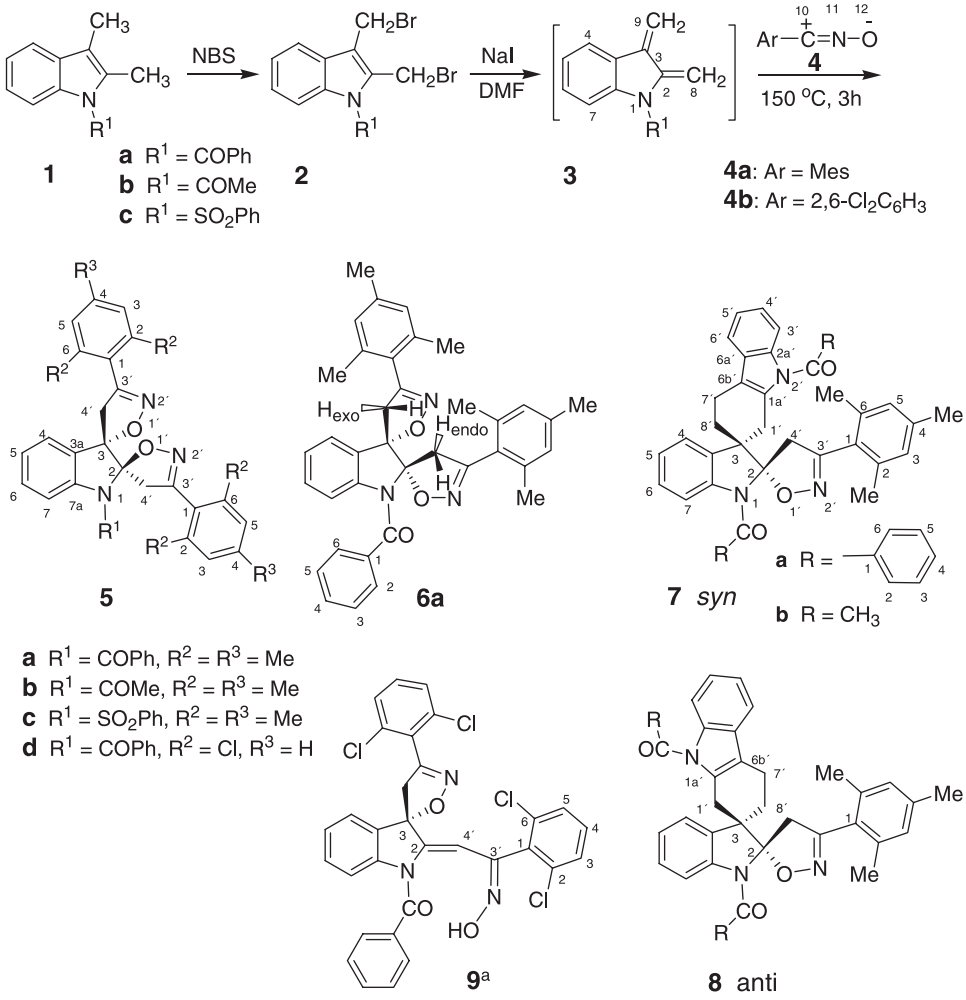

[a] The numbering of the substituent at C-2 is set analogously to the other derivatives.

Scheme 1. Preparation of *o*-QDMs **3**, their reaction with the stable nitrile oxides **4** and atom numbering at the reaction sites and the products **5**–**9**.

It is also worth mentioning that an exomethylenic dimeric [4+2] product was always isolated from the reaction of *N*-benzoyl indole *o*-quinodimethane with less reactive dienophiles.[16] Finally, from the reaction of quinodimethane **3a** with 2,6-dichlorobenzonitrile oxide, the oxime **9** was isolated in 13%, instead of the '*exo–syn*' dispiroindole.

2.1. Structure assignments by NMR spectra investigations

The assigned molecular structures of all new compounds **5**–**9** are based on rigorous spectroscopic analysis including IR, NMR (^{1}H, ^{13}H, COSY, NOESY, HETCOR and COLOC), MS and elemental analysis data.

Regarding the structure of the *anti* dispiroindoles **5** the assignment of **5a** is described. From the molecular ion at *m*/*z* 570 (corresponding to $M^+ + 1$) the conclusion could be drawn that **5a** is produced from the reaction of one molecule of **3a** with two molecules of mesitonitrile oxide, a fact that was also confirmed from the ^{13}C NMR spectrum where 29 different signals were observed (Table 1). Furthermore, from the C–H correlated spectrum in the saturated region, the presence of six mesito methyl groups, of two methylene groups with their carbons at 42.5 and 45.3 ppm and of two quaternary carbons at 92.1 and 107.4 ppm, connected with one and two heteroatoms, respectively, was established thus leading to the conclusion that a dispiroisoxazolinic indole derivative was formed.

Concerning the indole ring aromatic protons, COLOC correlations of the proton at δ 7.07 with the quaternary carbon at 130.9 ppm and of the proton at δ 7.46 with the quaternary carbon at 141.9 ppm and with CH carbon at 129.7 ppm were found. The first methylene group protons (δ 3.48 and 4.24) correlate with carbon at 158.0, whereas only the proton at δ 3.48 correlates with carbon at 130.9 ppm, indicating the position of methylene group (3-C4′) and the *exo* orientation of this proton, being coplanar with C-3a. The second methylene group protons (δ 3.91 and 4.07) correlate with carbon at 158.9. In addition, the correlation between proton at δ 4.07 and carbon at 92.1 ppm indicates the *endo* orientation of this proton. The *endo–exo* orientation of the methylene protons refers towards or in reverse to the neighbor isoxazoline ring (Scheme 1). The *o*-aromatic protons of CO-Ph group are deshielded (δ 7.70) and are easily distinguished from the rest of the aromatics. The COSY and COLOC correlations of these protons with the

Table 1. ^{1}H, ^{13}C and COLOC NMR data for compound **5a**

Position[a]	C	H[b]	COLOC[c]
2	107.4		
3	92.1		
3a	130.9		
4	123.6	7.46 (d, 7.8)[d]	141.9, 129.7
5	124.2	7.07 (m)[d]	130.9
6	129.7	7.00 (m)[d]	123.6
7	115.3	6.05 (d, 7.6)	
7a	141.9		
1-(CO)	168.7		
1-(1)	135.5		
1-(2,6)	128.8	7.70 (m)	168.7, 132.1
1-(3,5)	128.9	7.45 (m)[d]	135.5
1-(4)	132.1	7.57 (m)	128.8
2-(3′)	158.9		
2-(4′)	42.5	4.07 (d, 18.8)[e]	158.9, 92.1
		3.91 (d, 18.8)	158.9
2-(1)[f]	125.3		
2-(2,6)	137.7		
2-(3,5)	128.9	6.92 (s)	125.3, 21.1, 20.6
2-(4)	139.3		
2-(Me-2,6)	20.6	2.48 (s)	137.7, 128.9
2-(Me-4)	21.1	2.32 (s)	139.3, 128.9
3-(3′)	158.0		
3-(4′)	45.3	4.24 (d, 18.8)[e]	158.0, 92.1
		3.48 (d, 18.8)	158.0, 130.9
3-(1)[f]	125.2		
3-(2,6)	136.9		
3-(3,5)	128.9	6.95 (s)	125.2, 21.1, 20.3
3-(4)	139.0		
3-(Me-2,6)	20.3	2.38 (s)	136.9, 125.2, 128.9
3-(Me-4)	21.1	2.30 (s)	139.0, 128.9

[a] For carbon numbering see Scheme 1. The first number refers to indole ring position, the number in parenthesis refers to the substituent.
[b] Multiplicities and coupling constants (in Hertz) in parentheses.
[c] Long range ($^{2}J_{C-H}$ and $^{3}J_{C-H}$) correlations between the protons on the left and the carbons stated on this column.
[d] Overlaped multiplets, distinguished by homo- and hetero-COSY.
[e] In the order of *endo*, *exo* orientation.
[f] The mesito groups may be interchanged.

rest of aromatic protons and carbons lead to their assignment (Table 1). The two singlets at δ 6.92 and 6.95 belong to mesito groups and correlate with the aromatic and methyl carbons. By combination of these data the carbon sequence given in Scheme 1 for compound **5a** can be proposed.

In an analogous manner the structure assignment of the '*syn*' dispiroindole derivative **6a** was possible.

The assignment of **5a** to the'*exo–anti*' and of **6a** to the '*exo–syn*' addition product, respectively, was made in conjunction with the crystallographic results obtained[10] in the case of dispiroisoxazoline derivatives **12** and **13** (Scheme 2), where by analogy to **12**, the isomer, which is faster moving on TLC with a lower melting point corresponds to the '*exo–anti*' addition product **5a**.

Concerning the assignment of the dispiro derivative **7a** it was supported by the following data. The molecular ion at *m/z* 655 indicated the presence of two molecules of indole quinodimethane reacting with one molecule of mesitonitrile oxide. This was confirmed from the C–H correlated spectrum, where in the saturated region four methylene groups with their carbons resonating at 18.3, 27.9, 29.6 and 39.7, three methyl groups at 20.8 and 21.1 ppm (2:1) and two quaternary carbons at 50.7 and 110.5 ppm were observed. The quaternary carbon at 110.5 ppm, the methylene carbon at 39.7 ppm and the quaternary carbon at 157.3 could be attributed to a spiro isoxazoline ring, most likely formed from the quinodimethane exomethylene group next to the nitrogen, on account of the analogous chemical shifts observed for **5a** and **6a** (see also Section 2.2). In addition, the COLOC correlations observed between the carbon resonating at 157.3 ppm with the methylene group protons (δ 3.50 and 4.10) and between the carbon at 110.5 ppm with the methylene proton at δ 4.10 supported the formation of this isoxazoline ring.

Concerning the three remaining methylene groups, the one with its carbon at 27.9 ppm gave a very narrow AB system ($\nu_A = 3.24$, $\nu_B = 3.27$, $J_{AB} = 18.4$ Hz), whereas the remaining two at 29.6 and 18.3 ppm gave a complicated NMR spectrum thus indicating their vicinity.[17] Obviously, the methylene group with its carbon resonating at 29.6 ppm should be assigned to C-7′ next to aromatic indole ring. Moreover, all three methylene group protons gave COLOC correlations with carbon at 117.5 ppm. From these COLOC data the conclusion could be drawn that the second exomethylene group was used for the formation of a [4+2] *o*-quinodimethane dimmer creating thus the cyclohexene ring of compound **7** or **8**, from *syn* or *anti* approaching of the QDM moiety excluding thus all other possible adducts.

Finally, the assignment of oxime **9** was possible on account of the following data. From the combination of the molecular ion in mass spectrum with the 25 different carbon signals in the ^{13}C NMR, it was concluded that compound **9** was formed from one molecule of **3a** with two molecules of 2,6-dichlorobenzonitrile oxide. Furthermore, from the C–H correlated spectra in the saturated region the presence of only one methylene group and of a quaternary carbon at 88.2 ppm indicated the formation of only one isoxazoline ring. In addition, the methylene group protons gave COLOC correlations with the quaternary carbons at 156.2, 171.4, 128.7 and 88.2, whereas the indole ring proton at δ 7.42 is correlated with the quaternary carbon at 136.3 indicating thus the position of the isoxazoline ring. Concerning the addition of the second nitrile oxide molecule, the presence in the infrared spectrum of a hydroxyl at 3390 cm^{-1}, of a quaternary carbon at 171.4 ppm and of a proton at δ 6.45 (with its carbon resonating at 105.2 ppm), correlating with carbons at 171.4 and 159.1 ppm, led us to the structure **9**. Moreover, this structure was supported by the presence of a hydrogen bond between the hydroxyl proton at δ 9.27 and the amide oxygen (*N*–C=O at 165.3 ppm), as was revealed from their COLOC correlation. The stabilization of the COPh conformation, almost perpendicular to the indole ring, due to this hydrogen bond results to the very low field shift (δ 8.26) of indole proton H7 (Fig. 5).

2.2. Computational methods

Searching for the stereoselectivity reasons and since the X-ray crystallographic data for the quinodimethane adducts of **11** were available,[10] we attempted to investigate the reactions of *o*-QDMs **3** and **11** with mesito- and 2,6-dichlorobenzonitrile oxides (**4**) by studying the FMO

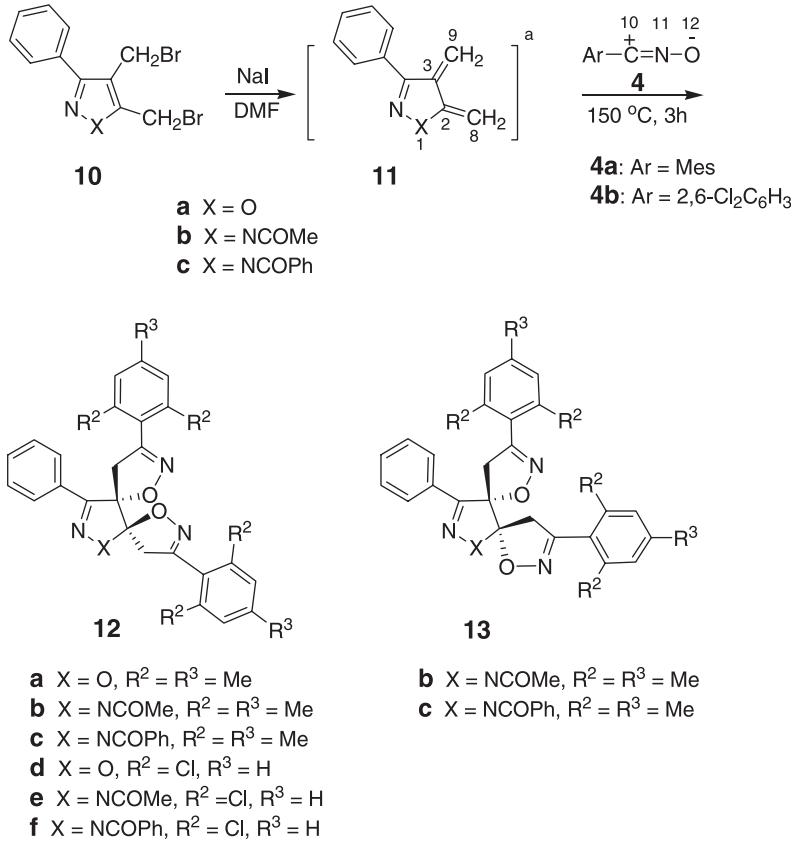

[a] The carbon numbering is analogous to QDM **3**.

Scheme 2. Preparation of *o*-QDMs **11** and their reaction with the nitrile oxides **4**.

interactions and the transition structures of the intermediates (AM1).

Experimentally, the *exo* addition products were isolated from the reaction of *o*-QDMs **3a–c** and **11a–c** with the nitrile oxides **4a–b**. We take for granted that the initial formation of the diene moiety is synchronous. In order to investigate the '*endo–exo*' and '*syn–anti*' addition selectivity of nitrile oxides to the two exomethylenic groups, the transition structures (TS) of the successive adducts at bonds $C_2{=}C_8$ and $C_3{=}C_9$ were located and examined in connection with HOMO–LUMO interactions of the reactants. Full geometry optimizations were carried out for nitrile oxides **4** and *o*-QDMs **3** and **11** as well as for the possible adducts at the AM1 level of theory. For each located TS after complete optimization only one negative eigenvalue was calculated corresponding to one imaginary frequency about 600–620 cm^{-1} and assigned to the new forming bonds[18] at methylene carbons C-8 or C-9. In Table 2 are presented the calculated HOMO–LUMO energies and the orbital coefficients (eigenvectors) for the atoms involved in the [2+3] cycloaddition reaction.

According to FMO interactions the additions of nitrile oxides **4a** and **4b** to *o*-QDMs **3** (Fig. 1) and **11** are predicted to be $HOMO_{(QDM)}$–$LUMO_{(dipole)}$ controlled, except in the case of QDM **11a**, where the addition of mesitonitrile oxide is predicted to be $HOMO_{(dipole)}$ controlled. The opposite attacking process is predicted to be energetically disfavored by 17.89 and 40.75 kcal/mol for **4a** and **4b**, respectively (Table 3). Looking at the $\Delta E(L_{dipole})$ values in Table 3, we notice that in all cases there is a difference of ~0.5 eV (~11.5 kcal/mol) favoring the reaction with nitrile oxide **4b**, validating the argument that **4b** is more reactive than **4a**.

In order to examine the *exo* selectivity of the reaction we carried out AM1 calculations for locating the TS for *exo* and *endo* addition of both nitrile oxides **4** to compound **3a** (Figs. 2 and 3). From Figure 2 it is observed that the new forming bond C_8–C_{10} (or C_9–C_{10}) is shorter than the second one C_2–O_{12} (or C_3–O_{12}) supporting the hypothesis of great asynchronicity in the above dipolar cycloaddition. In the case of *exo* approaching of **4a** to **3a** the C_8–C_{10}-Ar angle was calculated to be 109.1° in **TS1** and the C_9–C_{10}-Ar angle 111.2° in **TS2**, whereas for the *exo* approaching of **4b** to **3a** the corresponding angles were calculated to be 107.4° (**TS3**) and 110.4° (**TS4**), respectively. To the contrary, in *endo* approaching of **4a** to $C_2{=}C_8$ bond of **3a** the C_2–C_{10}-Ar angle was increased to 122.0° (**TS5**) and to $C_3{=}C_9$ bond the C_3–C_{10}-Ar angle was increased to 121.8° (**TS6**). Analogous angle increase was calculated for **4b** approach (**TS7–TS8**) revealing an increasing Van der Waals interaction. In addition, the $\Delta\Delta H^{\#}$ differences between the corresponding activation energies of *endo–exo* TS is 8.42 and 2.54 kcal/mol for the reaction of **3a** with **4a** at $C_2{=}C_8$ and $C_3{=}C_9$, respectively, and 8.50 and 4.46 kcal/mol for the reaction of **3a** with **4b** (Figs. 2 and 3). The energy differences between the $C_2{=}C_8$ and $C_3{=}C_9$ approaches can be attributed mostly to the Van der Waals interaction of CO-Ph substituent of **3a**. The energy profiles of the reactions are depicted in Figure 4.

Table 2. Calculated HOMO–LUMO energies (eV) and orbital coefficients (eigenvectors) for the atoms involved in new bond formations[a] for the reaction of *o*-QDMs **3a–c** and **11a–c** with nitrile oxides **4a** and **4b** (in gas phase at 298 K, AM1)

Comp.	HOMO	LUMO
3a	−8.396[b]	−0.328
C-8	0.4242[c]	0.2708
C-2	0.2163	−0.1508
C-3	−0.1838	−0.2996
C-9	−0.3646	0.4812
3b	−8.468	−0.381
C-8	−0.4263	−0.2654
C-2	−0.2267	0.1422
C-3	0.1910	0.2954
C-9	0.3713	−0.4798
3c	−8.646[b]	−0.391[d]
C-8	−0.4052	0.3329
C-2	−0.1987	−0.2116
C-3	0.2128	−0.3145
C-9	0.3933	0.5025
11a	−9.066	−0.652
C-8	0.4461	−0.3705
C-2	0.2518	0.2187
C-3	−0.2278	0.3085
C-9	−0.3929	−0.5134
11b	−8.598[b]	−0.590
C-8	−0.4664	0.2931
C-2	−0.2466	−0.1539
C-3	0.1812	−0.2654
C-9	0.3618	0.4565
11c	−8.602	−0.580
C-8	−0.4610	0.2793
C-2	−0.2435	−0.1475
C-3	0.1821	−0.2628
C-9	0.3617	0.4510
4a	−9.053[b]	−0.447
C-10	−0.3114	−0.2249
N-11	−0.2572	0.3454
O-12	0.4368	−0.2114
4b	−9.548	−0.943
C-10	0.3826	−0.1833
N-11	0.2637	0.3274
O-12	−0.4947	−0.2097

[a] For atom numbering of the diene moiety and nitrile oxides see Scheme 2.
[b] HOMO–LUMO energies (eV).
[c] Orbital coefficients (eigenvectors).
[d] NN–LUMO.

For the same type of reactions at the same temperature the factor $T\Delta S^{\#}$ is approximately the same, so $\Delta\Delta H^{\#}$ differences could be referred to as the $\Delta\Delta G^{\#}$ differences for Gibbs free energies of the TS.

Studying the MO coefficients in Table 2 the first attacking position of nitrile oxides can be predicted. The p_z orbital coefficients for the $C_2{=}C_8$ atoms of the reacting double bond of QDMs **3** and **11** are larger than those of the $C_3{=}C_9$ atoms. As a consequence, the $C_2{=}C_8$ bond most probably should be the first target for nitrile oxide addition. By examination of the corresponding TS for the reaction at the two different double bonds the same conclusion is extracted, since the addition at $C_2{=}C_8$ bond has 3.72 kcal/mol lower activation energy than the corresponding addition at $C_3{=}C_9$ bond (Fig. 4). This energy difference gives via the Boltzmann distribution equation a ratio of 536:1 preference at $C_2{=}C_8$ over $C_3{=}C_9$ (C_2/C_3) for a kinetically controlled reaction. An analogous preference for $C_2{=}C_8$ addition is predicted for all cycloadditions as presented in Table 4. For compound **3c** the preference for the first addition is reduced to 79:1. This can be attributed to the orientation of the N–SO_2-Ph group perpendicularly to the indole ring, so the approach to both double bonds is undisturbed from the opposite site of indole ring.

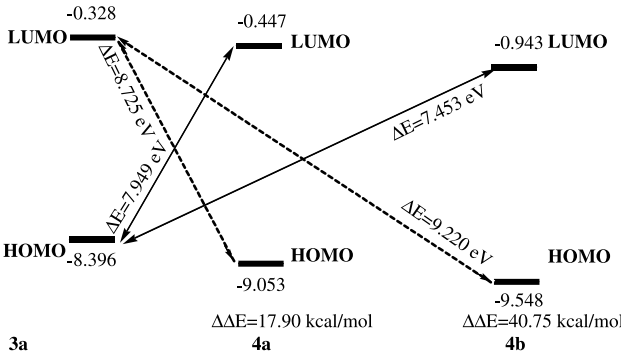

Figure 1. Molecular orbital correlation diagram for the interaction of *o*-QDM **3a** with the stable nitrile oxides **4a** and **4b**.

Concerning the *syn*/*anti* addition of the second nitrile oxide molecule at $C_3{=}C_9$ bond the energies and activation parameters for the transition structures have been calculated and presented in Table 5. From the $\Delta\Delta H^{\#}$ values a slight preference of *anti* over *syn* addition is always predicted for kinetically controlled reactions. The nitrile oxide **4b** is reactive enough to follow this reaction path and tries to approach and react to both reaction sites almost simultaneously, the *syn* approaching, however, being stereochemically disfavored. In agreement with this theoretical study, experimentally only the *anti* final products were isolated (Table 6). Nevertheless, from the reaction of **3a** with **4b** compound **9** was also isolated, possibly produced by almost simultaneous *syn* addition of two molecules of **4b** at reaction sites $C_2{=}C_8$ and $C_3{=}C_9$, respectively. As we noticed before, there is a great asynchronicity in the formation of the bonds C_8–C_{10} and C_2–O_{12} (see Fig. 2, **TS1**). Before the isoxazoline ring closure is completed at $C_2{=}C_8$ a second molecule of **4b** reacts at $C_3{=}C_9$, with *syn* or *anti* addition, since the energy difference between them is practically negligible. In the $C_3{=}C_9$ *syn* adduct, the bulky substituent at C-8 cannot be accommodated easily and fast between the two other substituents and finally oxygen abstracts, possibly via a free radical process, a hydrogen atom from the nearby methylene group giving the oxime **9**, depicted in Figure 5, which is 5.4 kcal more stable than the corresponding bis adduct **6d**.

Table 3. Energy differences for the various HOMO–LUMO interactions between quinodimethanes (**3a–c** and **11a–c**) and nitrile oxides **4a–b** (in gas phase at 298 K, AM1)

Reaction with			4a			4b		
QDM	HOMO	LUMO	$\Delta E(L_{dipole})$[a]	$\Delta E(H_{dipole})$	$\Delta\Delta E$[b]	$\Delta E(L_{dipole})$	$\Delta E(H_{dipole})$	$\Delta\Delta E$
3a	−8.396	−0.328	7.949	8.725	17.89	7.453	9.220	40.75
3b	−8.468	−0.381	8.021	8.672	15.01			
3c	−8.646	−0.391	8.199	8.662	10.68			
11a	−9.066	−0.652	8.619	8.401	−5.03	8.123	8.896	17.83
11b	−8.598	−0.590	8.151	8.463	7.19	7.655	8.958	30.05
11c	−8.606	−0.579	8.159	8.474	7.26	7.663	8.969	30.12

[a] $\Delta E(L_{dipole}) = E(LUMO_{dipole}) - E(HOMO_{QDM})$; $\Delta E(H_{dipole}) = E(HOMO_{dipole}) - E(LUMO_{QDM})$, (in eV/mol).
[b] $\Delta\Delta E = \Delta E(H_{dipole}) - \Delta E(L_{dipole})$, (in kcal/mol, 1 eV = 23.06 kcal/mol).

On the other hand, since the nitrile oxide **4a** is less reactive than **4b**, there is enough time to accommodate the groups of substituents after the first addition in $C_2{=}C_8$ bond. As a result, the second nitrile oxide molecule can approach from both sites giving '*exo–syn*' and '*exo–anti*' addition products. Considering the thermodynamics of the reaction and since reaction times were prolonged and therefore the reactions were thermodynamically controlled, the $\Delta\Delta H^o$ values of '*exo–syn*' and '*exo–anti*' addition products should also be taken into consideration. From the $\Delta\Delta H^o$ values given in Table 5 a small preference of '*exo–anti*' over '*exo–syn*' addition can be anticipated. In connection with the previous aspect of monoproduct accommodation both *syn* and *anti* products are derived. Experimentally, this was observed in the case of the QDMs **3a**, **11b** and **11c**. However, in the case of QDMs **3c** and **11a**, because of the higher values of $\Delta\Delta H^{\#}$ and (or) $\Delta\Delta H^o$ (Table 5a), '*exo–anti*' products were only isolated (Table 6).

Although we did not take into account the solvent effect, the above results show a good approximation with the experimental ones. In all computations presented in Table 5 the approaching of nitrile oxide **4a** takes place to the fully relaxed and energy minimized monoadduct, a situation that most probably is true only in the case of **4a**. Moreover, the formation of product **7** supports the prediction that the cycloaddition begins at $C_2{=}C_8$ followed by the addition of a second molecule of *o*-QDM at $C_3{=}C_9$. This is a consequence of the smaller reactivity of the nitrile oxide **4a** in comparison to **4b**.

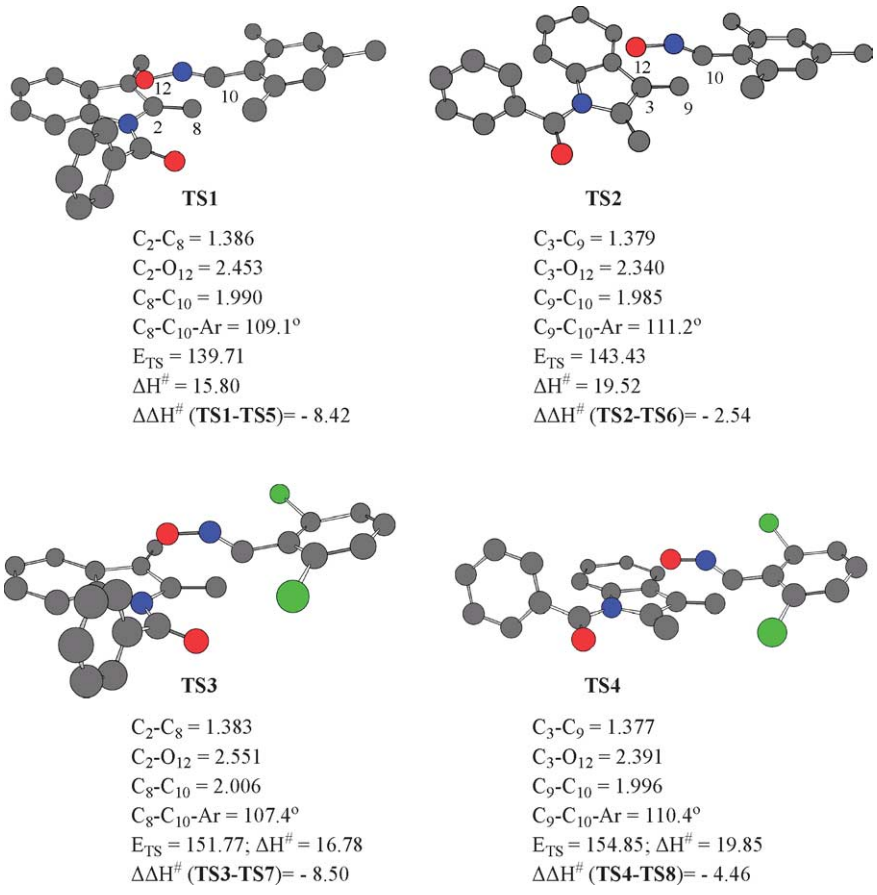

Figure 2. *exo* Transition structures optimized at AM1 level for the interaction of *o*-QDM **3a** with the stable nitrile oxides **4a** (**TS1**, **TS2**) and **4b** (**TS3**, **TS4**) at $C_2{=}C_8$ and at $C_3{=}C_9$ double bonds. $\Delta\Delta H^{\#}$ is the difference of $\Delta H^{\#}$ between the *exo* and *endo* approaching in the TS (see also Fig. 3). All bond lengths are in angstroms (Å), bond angles in degrees (°), energies in kcal/mol. For the numbering of reacting atoms see Scheme 1.

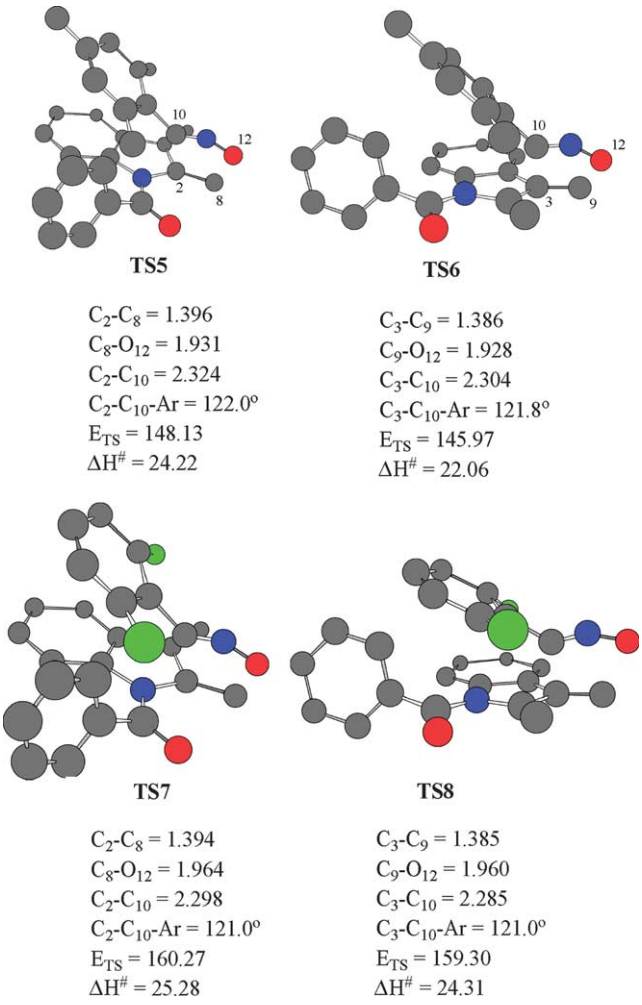

Figure 3. *endo* Transition structures for the interaction of *o*-QDM **3a** with the stable nitrile oxides **4a** and **4b** at C_2=C_8 and C_3=C_9 double bonds (AM1).

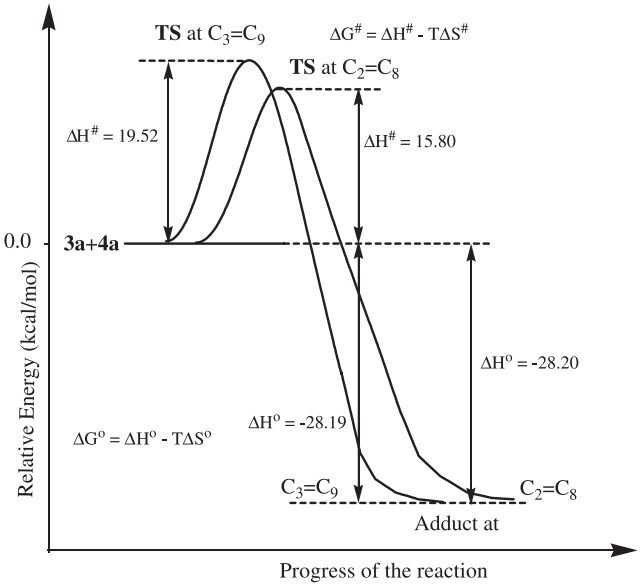

Figure 4. Reaction coordinate diagram of potential energy surface for the reaction **3a**+**4a** (*exo* monoadduct) at the two reaction sites C_2=C_8 and C_3=C_9 (energies in kcal/mol).

3. Conclusion

In conclusion, we have studied the reaction of some indole *o*-quinodimethanes with stable nitrile oxides **4**. Although these nitrile oxides are short lived at high temperatures and comparatively less reactive, it is remarkable that they reacted with the transient intermediate indole *o*-quinodimethanes giving in all cases the otherwise inaccessible *anti* indole dispiroisoxazolines, as the main or the only reaction products. In the case of reaction of quinodimethane **3a** with **4a** the '*exo–syn*' dispiroisoxazoline **6a** was also formed, whereas with **4b** the oxime **9** was isolated as a final product instead of **6d**. The very interesting indole quinodimethane dimerization and cycloaddition products **7** were also isolated. For all new compounds full assignment of proton and carbon NMR chemical shifts was achieved.

AM1 MO calculations support the experimental results concerning the '*endo–exo*' and '*syn–anti*' preference. The regioselectivity of the reactions is in accordance with the regioselectivity reported for the additions of nitrile oxides to 1,1-disubstituted alkenes.[19] The first nitrile oxide approaches the C_2=C_8 group freely from both sites only in *exo* configuration. The second nitrile oxide moiety approaches the C_3=C_9 bond preferentially in '*exo–anti*' configuration to the previously inserted group, as it was concluded from the X-ray structures[10] of adducts **12** and **13**.

4. Experimental

4.1. General

Melting points were measured on a Kofler hot-stage and are uncorrected. Column chromatography was carried out using Merck silica gel. Petroleum ether refers to the fraction boiling between 60 and 80 °C. NMR spectra were recorded at rt on a Bruker AM 300 spectrometer at 300 MHz for ^{1}H and 75 MHz for ^{13}C, respectively, using $CDCl_3$ as solvent. Chemical shifts are expressed in δ values (ppm) relative to TMS as internal standard for ^{1}H and relative to TMS (0.00 ppm) or to $CDCl_3$ (77.05 ppm) for ^{13}C NMR spectra. Coupling constants ^nJ are reported in Hertz. IR spectra were recorded on a Perkin-Elmer 297 spectrometer and are reported in wave numbers (cm^{-1}). Low-resolution electron impact mass spectra (EIMS) were obtained on a VG TS-250 instrument and elemental analyses performed with a Perkin-Elmer 2400-II CHN analyzer. Structural assignments of the derived compounds were established by analysis of their IR, MS and NMR spectra (^{1}H, ^{13}C, COSY, NOESY, HETCOR and COLOC). The MO calculations for minimum energy conformation of compounds were computed with the AM1 method as implemented in the MOPAC package[20] version 6.3. All stationary points were refined by minimization of the gradient norm of the energy to at least 0.005 kcal/mol. The ^{13}C and ^{1}H NMR data of compounds **5b–d**, **6a**, **7a–b** and **9** are summarized and presented also for comparison in Tables S1 and S2 as supplementary data in supporting information.

Table 4. Calculated energies of formation ΔH_f[a] and activation parameters for the *exo* transition structures and products for the reactions of *o*-QDMs **3a–c** and **11a–c** to form monoadduct: (a) with mesitonitrile oxide and (b) with 2,6-dichlorobenzonitrile oxide (in gas phase, 298 K, AM1)

	Addition at C_2=C_8					Addition at C_3=C_9					
QDM	$\Sigma\Delta H_{f(r)}$	$\Delta H_{f(p)}$	ΔH^{o}[b]	E_{TS}[c]	$\Delta H^{\#}$[d]	$\Delta H_{f(p)}$	ΔH^{o}	E_{TS}	$\Delta H^{\#}$	$\Delta\Delta H^{\#}$[e,f]	C_2/C_3[g]
(a)											
3a	123.91	95.71	−28.20	139.71	15.80	95.72	−28.19	143.43	19.52	−3.72	536
3b	87.69	59.55	−28.14	104.37	16.68	59.55	−28.14	107.26	19.58	−2.90	134
3c	89.45	63.49	−25.96	107.47	18.02	61.85	−27.60	110.06	20.61	−2.59	79
11a	135.36	97.98	−37.38	152.11	16.75	107.37	−27.99	155.93	20.58	−3.83	645
11b	128.20	99.86	−28.34	144.34	16.14	99.26	−28.94	147.99	19.79	−3.65	476
11c	164.77	136.62	−28.15	180.98	16.21	135.94	−28.83	184.92	20.50	−4.29	1404
(b)											
3a	134.99	107.07	−27.92	151.77	16.78	105.87	−29.12	154.85	19.86	−3.08	182
11a	146.44	108.23	−38.21	163.65	17.21	117.42	−29.02	167.42	20.98	−3.77	583
11b	139.28	111.16	−28.12	156.71	17.43	109.38	−29.90	159.46	20.18	−2.75	104
11c	175.85	147.94	−27.91	193.28	17.43	146.06	−29.79	196.46	20.61	−3.18	215

[a] ΔH_f for the reactants (in kcal/mol): **3a**=81.33; **3b**=45.11; **3c**=46.87; **11a**=92.78; **11b**=85.62; **11c**=122.19; **4a**=42.58; **4b**=53.66.
[b] $\Delta H^{o}=\Delta H_{f(p)}-\Sigma\Delta H_{f(r)}$, where $\Sigma\Delta H_{f(r)}=\Delta H_{f(n.o)}+\Delta H_{f(QDM)}$,(r=reactants, p=products, n.o=nitrile oxide).
[c] E_{TS} is the calculated ΔH_f for the transition state.
[d] $\Delta H^{\#}=E_{TS}-\Sigma\Delta H_{f(r)}$.
[e] $\Delta\Delta H^{\#}=\Delta H^{\#}_{(\text{adduct at } C_2=C_8)}-\Delta H^{\#}_{(\text{adduct at } C_3=C_9)}$ is the relative activation energy.
[f] A negative value means a more stable TS at C_2=C_8 and the corresponding adduct is favored kinetically.
[g] C_2/C_3 is the relative calculated ratio of adducts at C_2=C_8 versus C_3=C_9 by the Boltzmann equation for equilibrium distribution.

Table 5. Calculated energies ΔH_f and activation parameters for the transition structures for the reactions of monoadducts of *o*-QDMs **3** and **11** at C_2=C_8 with a second molecule of (a) mesitonitrile oxide and (b) 2,6-dichlorobenzonitrile oxide in *exo–syn* and *exo–anti* configuration (in gas phase, at 298 K, AM1)[a]

QDM	$\Sigma\Delta H_{f(r)}$	$\Delta H_{f(p)}$	ΔH^{o}	E_{TS}	$\Delta H^{\#}$	$\Delta H_{f(p)}$	ΔH^{o}	E_{TS}	$\Delta H^{\#}$	$\Delta\Delta H^{ob}$	$\Delta\Delta H^{\#c}$
(a) Adduct of **4a** at C-2:			*exo–syn* addition at C-3				*exo–anti* addition at C-3				
3a	138.29	113.76	−24.53	160.17	21.88	109.02	−28.89	159.73	21.44	4.36	0.44
3b	102.13	77.69	−24.44	123.83	21.70	73.13	−29.00	123.67	21.54	4.56	0.16
3c	106.07	78.27	−27.80	128.80	22.73	74.45	−31.62	127.89	21.82	3.82	0.91
11a	140.56	113.12	−27.44	163.04	22.48	108.99	−31.57	161.07	20.51	4.13	1.97
11b	142.44	115.92	−26.52	164.30	21.86	111.87	−30.57	163.40	20.96	4.05	0.90
11c	179.20	152.49	−26.71	200.95	21.75	148.04	−31.16	200.26	21.06	4.45	0.69
(b) Adduct of **4b** at C-2:			*exo–syn* addition at C-3				*exo–anti* addition at C-3				
3a	160.73	135.34	−25.39	182.98	22.25	131.23	−29.50	182.85	22.12	4.11	0.13
11a	161.89	133.96	−27.93	184.59	22.70	129.79	−32.10	183.00	21.11	4.17	1.59
11b	164.82	137.94	−26.88	187.21	22.39	133.49	−31.33	186.70	21.88	4.45	0.51
11c	201.60	174.66	−26.94	223.70	22.10	171.10	−30.50	223.55	21.95	3.55	0.15

[a] The symbols have the same meaning as in Table 4.
[b] $\Delta\Delta H^{o}=\Delta H^{o}_{(syn\ \text{product})}-\Delta H^{o}_{(anti\ \text{product})}$, relative energy of formation. A positive value means the corresponding *anti* product is more stable and is favored thermodynamically.
[c] $\Delta\Delta H^{\#}=\Delta H^{\#}_{(syn\ \text{product})}-\Delta H^{\#}_{(anti\ \text{product})}$ relative activation energy. A positive value means a more stable TS for the *anti* approach and the corresponding adduct is favored kinetically.

4.2. Reaction of 1-benzoyl-2,3-bis(bromomethyl)indole (2a) with mesitonitrile oxide. General procedure

Sodium iodide (0.30 g, 2.0 mmol) was added in one portion to a stirred solution of 1-benzoyl-2,3-bis(bromomethyl)indole (**2a**) (0.41 g, 1.0 mmol) and mesitonitrile oxide (0.335 g, 2.1 mmol) in dry DMF (30 mL). The reaction mixture was stirred under reflux (153 °C) for 3 h, the solvent was evaporated under reduced pressure, and the residue was extracted with dichloromethane. The suspension was washed with saturated aqueous sodium hydrogen sulfite and then with water. The organic layer was separated, dried (Na_2SO_4) and evaporated under reduced pressure. The residue was purified by column chromatography on silica gel using petroleum ether/EtOAc as eluent, slowly increasing the polarity to give in order of elution.

Table 6. The various addition products with their yields (%) from the studied reactions

Reactants		Products (%)				
3a+**4a**	**5a**	20	**6a**	7	**7a**	13
3a+**4b**	**5d**	25			**9**	13
3b+**4a**	**5b**	29			**7b**	18
3c+**4a**	**5c**	46				
11a+**4a**[a]	**12a**	31				
11a+**4b**	**12d**	43				
11b+**4a**	**12b**	19	**13b**	15		
11b+**4b**	**12e**	37				
11c+**4a**	**12c**	21	**13c**	19		
11c+**4b**	**12f**	46				

[a] Reactions with QDMs **11** were carried out at 120–130 °C for 2 h in DMF (Ref. 10).

4.2.1. (3′*S*,5*R* or 3′*R*,5*S*)-1′-Benzoyl-3,3″-dimesityl-1′*H*,4*H*,4″*H*-dispiro[isoxazole-5,2′-indole-3′,5″-isoxazole] 5a.

0.115 g, 20% Yield, white solid, mp 184–185 °C (EtOH); IR (Nujol) ν_{max}: 1660 cm^{-1}. ^1H NMR: 2.30 (s, 3H, 3-(Me-4)), 2.32 (s, 3H, 2-(Me-4)), 2.38 (s, 6H, 3-(Me-2,6)), 2.48 (s, 6H, 2-(Me-2,6)), 3.48 (d, J=18.8 Hz, 1H, *exo*-3-C(4′)), 3.91 (d, J=18.8 Hz, 1H, *exo*-2-C(4′)), 4.07 (d, J=18.8 Hz, 1H, *endo*-2-C(4′)), 4.24 (d, J=18.8 Hz, 1H, *endo*-3-C(4′)), 6.05 (d, J=7.6 Hz, 1H, C(7)), 6.92 (s, 2H, 2-C(3,5)), 6.95 (s, 2H, 3-C(3,5)), 7.00 (m, 1H, C(6)), 7.07

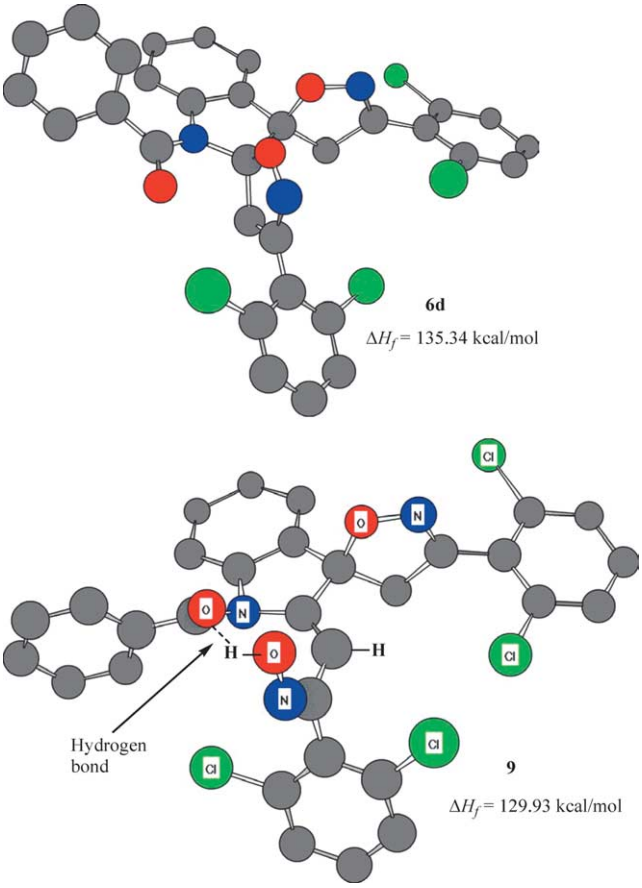

Figure 5. Energy minimized molecular models for compound **9**, where the hydrogen bond between C=*O*···*H*O–N can be distinguished, and for the corresponding bis adduct **6d**.

(m, 1H, C(5)), 7.45 (m, 2H, 1-C(3,5)), 7.46 (d, J=7.8 Hz, 1H, C(4)), 7.57 (m, 1H, 1-C(4)), 7.70 (m, 2H, 1-C(2,6)). ^{13}C NMR: 20.3 (3-(Me-2,6)), 20.6 (2-(Me-2,6)), 21.1 (2-(Me-4)), 21.1 (3-(Me-4)), 42.5 (2-(4′)), 45.3 (3-(4′)), 92.1 (3), 107.4 (2), 115.3 (7), 123.6 (4), 124.2 (5), 125.2 (3-(1)), 125.3 (2-(1)), 128.8 (1-(2,6)), 128.9 (1-(3,5)), 128.9 (2-(3,5)), 128.9 (3-(3,5)), 129.7 (6), 130.9 (3a), 132.1 (1-(4)), 135.5 (1-(1)), 136.9 (3-(2,6)), 137.7 (2-(2,6)), 139.0 (3-(4)), 139.3 (2-(4)), 141.9 (7a), 158.0 (3-(3′)), 158.9 (2-(3′)), 168.7 (1-(CO)). EIMS *m*/*z* (%) 570 (13, $M^{+\cdot}$+1), 464 (4), 450 (100), 434 (43), 408 (26), 221 (19), 105 (85), 77 (6). Anal. Calcd for $C_{37}H_{35}N_3O_3$ (569.67): C, 78.00; H, 6.19; N, 7.38%. Found: C, 77.81; H, 6.08; N, 7.47%.

4.2.2. 1′,9-Dibenzoyl-3″-mesityl-1,3,4,9-tetrahydro-1′*H*,4″*H*-dispiro[carbazole-2,3′-indole-2′,5″-isoxazole] 7a (or 8a). 0.085 g, 13% Yield, white solid, mp 248–250 °C (EtOH); IR (Nujol) ν_{max}: 1665, 1590 cm^{-1}. ^{1}H NMR: 2.03 (ddd, J=12.0, 4.0, 1.0 Hz, 1H, 3-C(8′)), 2.19 (ddd, J=12.0, 12.0, 5.0 Hz, 1H, 3-C(8′)), 2.30 (s, 3H, 2-(Me-4)), 2.53 (s, 6H, 2-(Me-2,6)), 2.66 (ddd, J=16.3, 12.0, 4.0 Hz, 1H, 3-C(7′)), 2.99 (ddd, J=16.3, 5.0, 1.0 Hz, 1H, 3-C(7′)), 3.24 (d, J=18.4 Hz, 1H, 3-C(4′)), 3.27 (d, J=18.4 Hz, 1H, 3-C(4′)), 3.50 (d, J=19.3 Hz, 1H, 2-C(4′)), 4.10 (d, J=19.3 Hz, 1H, 2-C(4′)), 6.07 (m, 1H, C(7)), 6.79 (m, 1H, C(5)), 6.85 (m, 1H, C(6)), 6.86 (m, 1H, C(4)), 6.92 (s, 2H, 2-C(3,5)), 7.00 (m, 1H, 3-C(3′)), 7.11 (m, 1H, 3-C(4′)), 7.23 (m, 1H, 3-C(5′)), 7.46 (m, 2H, 3-C(3,5)), 7.50 (m, 2H, 1-C(3,5)), 7.50 (m, 1H, 3-C(6′)), 7.55 (m, 1H, 1-C(4)), 7.62 (m, 1H, 3-C(4)), 7.68 (m, 2H, 1-C(2,6)), 7.76 (m, 2H, 3-C(2,6)). ^{13}C NMR: 18.3 (3-(8′)), 20.8 (2-(Me-2,6)), 21.1 (2-(Me-4)), 27.9 (3-(1′)), 29.6 (3-(7′)), 39.70 (2-(4′)), 50.7 (3), 110.5 (2), 114.7 (3-(3′)), 116.0 (7), 117.5 (3-(6b′)), 118.2 (3-(6′)), 122.7 (3-(5′)), 123.5 (5), 123.6 (4), 123.7 (3-(4′)), 126.0 (2-(1)), 127.4 (6), 128.8 (2-(3,5)), 128.9 (1-(3,5)), 128.9 (1-(2,6)), 128.9 (3-(3,5)), 129.5 (3-(2,6)), 131.2 (3-(6a′)), 132.0 (1-(4)), 132.9 (3-(4)), 134.8 (3-(1a′)), 135.1 (3a), 135.4 (1-(1)), 136.0 (3-(1)), 137.2 (3-(2a′)), 137.7 (2-(2,6)), 138.8 (2-(4)), 141.7 (7a), 157.3 (2-(3′)), 169.0 (1-(CO)), 169.1 (3-(CO)). EIMS *m*/*z* (%) 655 (<1, $M^{+\cdot}$), 640 (6), 450 (33), 392 (89), 105 (100), 77 (68). Anal. Calcd for $C_{44}H_{37}N_3O_3$ (655.78): C, 80.59; H, 5.69; N, 6.41%. Found: C, 80.75; H, 5.82; N, 6.34%.

4.2.3. (3′*R*,5*R* or 3′*S*,5*S*)-1′-Benzoyl-3,3″-dimesityl-1′*H*,4*H*,4″*H*-dispiro[isoxazole-5,2′-indole-3′,5″-isoxazole] 6a. 0.040 g, 7% Yield, white solid, mp 218–220 °C (EtOH); IR (Nujol) ν_{max}: 1655 cm^{-1}. ^{1}H NMR: 2.30 (s, 3H, 2-(Me-4)), 2.30 (s, 3H, 3-(Me-4)), 2.31 (s, 6H, 3-(Me-2,6)), 2.48 (s, 6H, 2-(Me-2,6)), 3.42 (d, J=18.5 Hz, 1H, *exo*-3-C(4′)), 3.44 (d, J=18.2 Hz, 1H, *exo*-2-C(4′)), 3.78 (d, J=18.5 Hz, 1H, *endo*-3-C(4′)), 4.11 (d, J=18.2 Hz, 1H, *endo*-2-C(4′)), 6.10 (m, 1H, C(7)), 6.92 (s, 2H, 2-C(3,5)), 6.92 (s, 2H, 3-C(3,5)), 6.99 (m, 1H, C(6)), 7.07 (m, 1H, C(5)), 7.45 (m, 2H, 1-C(3,5)), 7.45 (d, J=7.3 Hz, 1H, C(4)), 7.57 (m, 1H, 1-C(4)), 7.70 (m, 2H, 1-C(2,6)). ^{13}C NMR: 20.0 (3-(Me-2,6)), 20.2 (2-(Me-2,6)), 21.1 (2-(Me-4)), 21.1 (3-(Me-4)), 41.7 (2-(4′)), 47.7 (3-(4′)), 91.8 (3), 107.8 (2), 116.0 (7), 122.5 (4), 124.3 (5), 125.1 (3-(1)), 125.5 (2-(1)), 128.6 (2-(3,5)), 128.8 (3-(3,5)), 128.9 (1-(3,5)), 128.9 (1-(2,6)), 129.2 (6), 132.7 (3a), 132.4 (1-(4)), 135.2 (1-(1)), 136.5 (3-(2,6)), 137.7 (2-(2,6)), 139.0 (2-(4)), 139.4 (3-(4)), 141.8 (7a), 156.5 (3-(3′)), 156.8 (2-(3′)), 165.0 (CO). EIMS *m*/*z* (%) 569 (20, $M^{+\cdot}$), 449 (37), 433 (16), 408 (10), 105 (100), 77 (22). Anal. Calcd for $C_{37}H_{35}N_3O_3$ (569.67): C, 78.00; H, 6.19; N, 7.38%. Found: C, 78.13; H, 6.28; N, 7.27%.

4.3. Reaction of 1-acetyl-2,3-bis(bromomethyl)indole (2b) with mesitonitrile oxide

The reaction was carried out as described above with 1.0 mmol of 1-acetyl-2,3-bisbromomethylindole (**2b**) and 2.1 mmol of mesitonitrile oxide to afford after column chromatography in order of elution.

4.3.1. (3′*R*,5*S* or 3′*S*,5*R*)-1′-Acetyl-3,3″-dimesityl-1′*H*,4*H*,4″*H*-dispiro[isoxazole-5,2′-indole-3′,5″-isoxazole] 5b. White solid, mp 234–236 °C (EtOH), 0.147 g, 29% yield. IR (Nujol) ν_{max}: 1650 cm^{-1}. ^{1}H NMR: 2.29 (s, 3H, 2-(Me-4)), 2.30 (s, 3H, 3-(Me-4)), 2.33 (s, 6H, 2-(Me-2,6)), 2.38 (s, 6H, 3-(Me-2,6)), 2.51 (s, 3H, CO–Me), 3.18 (d, J=18.7 Hz, 1H, *exo*-3-C(4′)), 3.49 (d, J=19.1 Hz, 1H, *exo*-2-C(4′)), 4.34 (d, J=19.1 Hz, 1H, *endo*-2-C(4′)), 4.38 (d, J=18.7 Hz, 1H, *endo*-3-C(4′)), 6.91 (s, 2H, 2-C(3,5)), 6.92 (s, 2H, 3-C(3,5)), 7.20 (m, 1H, C(5)), 7.36 (m, 1H, C(6)), 7.45 (d, J=7.5 Hz, 1H, C(4)), 7.81 (br, 1H, C(7)). ^{13}C NMR: 19.9 (2-(Me-2,6)), 20.4 (3-(Me-2,6)), 21.1 (2-(Me-4)), 21.1 (3-(Me-4)), 25.0 (CO–Me), 44.9 (2-(4′)), 47.4 (3-(4′)), 92.7 (3), 106.3 (2), 116.2 (7), 123.3 (4), 124.9 (2-(1)), 125.0 (3-(1)), 125.1 (5), 128.7 (2-(3,5)), 129.0 (3-(3,5)), 130.3 (6), 131.0 (3a), 137.0 (2-(2,6)), 137.3 (3-(2,6)), 139.3 (2-(4)),

139.4 (3-(4)), 140.5 (7a), 158.5 (3-(3′)), 160.4 (2-(3′)), 169.2 (CO). EIMS *m/z* (%) 508 (13, $M^{+\cdot}$), 466 (10), 347 (32), 105 (85), 77 (100). Anal. Calcd for $C_{32}H_{33}N_3O_3$ (507.61): C, 75.71; H, 6.55; N, 8.28%. Found: C, 75.81; H, 6.38; N, 8.64%.

4.3.2. 1′,9-Diacetyl-3″-mesityl-1,3,4,9-tetrahydro-1′*H*,4″*H*-dispiro[carbazole-2,3′-indole-2′,5″-isoxazole] 7b (or 8b). White solid, mp 240–242 °C (EtOH), 0.096 g, 18% yield. ^{1}H NMR: 1.77 (m, 1H, 3-C(8′)), 2.02 (m, 1H, 3-C(8′)), 2.29 (s, 3H, 2-(Me-4)), 2.46 (s, 6H, 2-(Me-2,6)), 2.49 (m, 1H, 3-C(7′)), 2.55 (s, 3H, CO–Me), 2.72 (s, 3H, 3-(CO–Me)), 2.87 (m, 1H, 3-C(7′)), 3.28 (d, *J*=18.2 Hz, 1H, 3-C(4′)), 3.44 (d, *J*=18.6 Hz, 1H, 2-C(4′)), 3.49 (d, *J*=18.2 Hz, 1H, 3-C(4′)), 4.27 (d, *J*=18.6 Hz, 1H, 2-C(4′)), 6.89 (m, 1H, C(7)), 6.90 (m, 1H, C(4)), 6.90 (m, 1H, 3-C(4′)), 6.91 (s, 2H, 2-C(3,5)), 7.21 (m, 1H, C(6)), 7.31 (m, 1H, 3-C(5′)), 7.35 (m, 1H, 3-C(6′)), 7.37 (m, 1H, C(5)), 8.17 (m, 1H, 3-C(3′)). ^{13}C NMR: 18.0 (3-(8′)), 20.6 (2-(Me-2,6)), 21.0 (2-(Me-4)), 25.7 (1-COMe), 27.2 (3-COMe), 28.9 (3-(1′)), 29.4 (3-(7′)), 40.1 (2-(4′)), 50.4 (3), 110.1 (2), 115.2 (3-(3′)), 115.8 (7), 118.2 (3-(6′)), 118.2 (3-(6b′)), 123.3 (3-(5′)), 124.1 (4), 124.1 (5), 124.7 (3-(4′)), 125.7 (2-(1)), 128.1 (6), 128.9 (2-(3,5)), 129.0 (3-(6a′)), 133.2 (3-(1a′)), 135.6 (3a), 136.6 (3-(2a′)), 137.4 (2-(2,6)), 138.9 (2-(4)), 140.4 (7a), 157.9 (2-(3′)), 169.6 (1-(CO)), 169.7 (3-(CO)). EIMS *m/z* (%) 531 (3, $M^{+\cdot}$), 516 (10), 488 (22), 412 (5), 372 (90), 105 (100), 77 (67). Anal. Calcd for $C_{34}H_{33}N_3O_3$ (531.64): C, 76.81; H, 6.26; N, 7.90%. Found: C, 76.60; H, 6.38; N, 8.04%.

4.4. Reaction of 1-sulfonyl-2,3-bis(bromomethyl)indole (2c) with mesitonitrile oxide

The reaction was carried out as described above with 1.0 mmol of 1-sulfonyl-2,3-bisbromomethylindole (**2c**) and 2.1 mmol of mesitonitrile oxide to afford after column chromatography compound **5c**.

4.4.1. (3′*S*,5*R* or 3′*R*,5*S*)-3,3″-Dimesityl-1′-(phenylsulfonyl)-1′*H*,4*H*,4″*H*-dispiro[isoxazole-5,2′-indole-3′,5″-isoxazole] 5c. White solid, mp 126–128 °C (EtOH), 0.278 g, 46% yield. ^{1}H NMR: 2.26 (s, 6H, 3-(Me-2,6)), 2.28 (s, 3H, 2-(Me-4)), 2.30 (s, 3H, 3-(Me-4)), 2.42 (s, 6H, 2-(Me-2,6)), 3.03 (d, *J*=18.8 Hz, 1H, *exo*-3-C(4′)), 3.85 (d, *J*=18.8 Hz, 1H, *endo*-3-C(4′)), 4.00 (d, *J*=19.3 Hz, 1H, *exo*-2-C(4′)), 4.40 (d, *J*=19.3 Hz, 1H, *endo*-2-C(4′)), 6.88 (s, 2H, 2-C(3,5)), 6.92 (s, 2H, 3-C(3,5)), 7.15 (m, 1H, C(5)), 7.35 (m, 1H, C(6)), 7.37 (d, *J*=7.6 Hz, 1H, C(4)), 7.45 (m, 2H, 1-C(3,5)), 7.53 (m, 1H, 1-C(4)), 7.69 (d, *J*=8.3 Hz, 1H, C(7)), 8.07 (m, 2H, 1-C(2,6)). ^{13}C NMR: 20.1 (3-(Me-2,6)), 20.3 (2-(Me-2,6)), 21.1 (2-(Me-4)), 21.1 (3-(Me-4)), 46.8 (2-(4′)), 47.1 (3-(4′)), 93.0 (3), 108.2 (2), 114.4 (7), 123.5 (4), 124.8 (5), 124.5 (2-(1)), 124.8 (3-(1)), 127.7 (1-(2,6)), 128.8 (3-(3,5)), 128.9 (1-(3,5)), 128.9 (2-(3,5)), 130.2 (3a), 130.8 (6), 133.3 (1-(4)), 136.9 (3-(2,6)), 137.6 (2-(2,6)), 139.3 (2-(4)), 139.3 (3-(4)), 139.9 (7a), 140.3 (1-(1)), 158.0 (3-(3′)), 160.4 (2-(3′)). EIMS *m/z* (%) 605 (7, $M^{+\cdot}$), 463 (58), 319 (51), 157 (55), 103 (100), 77 (56). Anal. Calcd for $C_{36}H_{35}N_3O_4S$ (605.75): C, 71.38; H, 5.82; N, 6.94%. Found: C, 71.48; H, 5.66; N, 7.11%.

4.5. Reaction of 1-benzoyl-2,3-bis(bromomethyl)indole (2a) with 2,6-dichloronitrile oxide

The reaction was carried out as described above with 1.0 mmol of 1-benzoyl-2,3-bisbromomethylindole (**2a**) and 2.1 mmol of 2,6-dichloronitrile oxide to afford after column chromatography compound in order of elution.

4.5.1. (3′*R*,5*S* or 3′*S*,5*R*)-1′-Benzoyl-3,3″-bis(2,6-dichlorophenyl)-1′*H*,4*H*,4″*H*-dispiro[isoxazole-5,2′-indole-3′,5″-isoxazole] 5d. White solid, mp 233–235 °C (EtOH), 0.156 g, 25% yield. IR (Nujol) ν_{max}: 1660 cm^{-1}. ^{1}H NMR: 3.93 (d, *J*=19.1 Hz, 1H, *exo*-3-C(4′)), 3.95 (d, *J*=19.1 Hz, 1H, *endo*-3-C(4′)), 4.01 (d, *J*=19.2 Hz, 1H, *exo*-2-C(4′)), 4.26 (d, *J*=19.2 Hz, 1H, *endo*-2-C(4′)), 6.11 (m, 1H, C(7)), 7.07 (m, 1H, C(5)), 7.07 (m, 1H, C(6)), 7.30 (m, 1H, 3-C(4)), 7.36 (m, 1H, 2-C(4)), 7.41 (m, 2H, 3-C(3,5)), 7.45 (m, 2H, 2-C(3,5)), 7.48 (m, 2H, 1-C(3,5)), 7.58 (m, 1H, 1-C(4)), 7.62 (m, 1H, C(4)), 7.75 (m, 2H, 1-C(2,6)). ^{13}C NMR: 39.5 (2-(4′)), 40.7 (3-(4′)), 93.5 (3), 107.6 (2), 115.6 (7), 124.1 (4), 124.2 (5), 127.7 (2-(1)), 127.7 (3-(1)), 128.6 (1-(3,5)), 128.7 (2-(3,5)), 128.9 (1-(2,6)), 128.9 (3-(3,5)), 130.1 (3a), 130.2 (6), 131.0 (3-(4)), 131.4 (2-(4)), 132.2 (1-(4)), 135.3 (1-(1)), 135.3 (2-(2,6)), 135.7 (3-(2,6)), 143.2 (7a), 153.9 (3-(3′)), 154.7 (2-(3′)), 168.7 (1-(CO)). EIMS *m/z* (%) 629/627/625/623/621 (7, $M^{+\cdot}$), 505/503/501 (6), 467 (13), 465 (13), 345 (9), 331 (11), 214 (25), 196 (75), 171 (46), 105 (97), 77 (100). Anal. Calcd for $C_{31}H_{19}Cl_4N_3O_3$ (623.31): C, 59.73; H, 3.07; N 6.74%. Found: C, 59.54; H, 2.99; N, 6.83%.

4.5.2. (1*E*,2*Z*)-2-[(3*R*)-1-Benzoyl-3′-(2,6-dichlorophenyl)-4′*H*-spiro[indole-3,5′-isoxazol]-2(1*H*)-ylidene]-1-(2,6-dichlorophenyl)ethanone oxime 9. White solid, mp 200–202 °C (EtOH), 0.081 g, 13% yield. IR (Nujol) ν_{max}: 3400, 1660 cm^{-1}. ^{1}H NMR: 4.14 (d, *J*=16.8 Hz, 1H, 3-C(4′)), 4.17 (d, *J*=16.8 Hz, 1H, 3-C(4′)), 6.45 (s, 1H, 2-C(4′)), 7.27 (m, 1H, C(5)), 7.29 (m, 1H, 3-C(4)), 7.31 (m, 1H, 2-C(4)), 7.34 (m, 2H, 2-C(3,5)), 7.34 (m, 2H, 3-C(3,5)), 7.42 (m, 1H, C(6)), 7.49 (m, 2H, 1-C(3,5)), 7.52 (d, *J*=7.3 Hz, 1H, C(4)), 7.54 (m, 1H, 1-C(4)), 7.95 (m, 2H, 1-C(2,6)), 8.26 (d, *J*=8.1 Hz, 1H, C(7)), 9.27 (s, 1H, OH). ^{13}C NMR: 48.1 (3-(4′)), 88.2 (3), 105.2 (2-(4′)), 125.2 (5), 125.5 (7), 127.0 (2-(1)), 127.2 (1-(2,6)), 127.4 (6), 127.7 (3-(1)), 128.2 (2-(3,5)), 128.2 (3-(3,5)), 128.7 (3a), 128.9 (1-(3,5)), 130.4 (4), 131.2 (3-(4)), 131.7 (2-(4)), 132.1 (1-(4)), 134.2 (1-(1)), 135.0 (3-(2,6)), 135.5 (2-(2,6)), 136.3 (7a), 156.2 (3-(3′)), 159.1 (2-(3′)), 165.3 (1-(CO)), 171.4 (2). EIMS *m/z* (%) 629/627/625/623/621 (39, $M^{+\cdot}$), 329 (37), 214 (98), 196 (100), 171 (46), 105 (97). Anal. Calcd for $C_{31}H_{19}Cl_4N_3O_3$ (623.31): C, 59.73; H, 3.07; N 6.74%. Found: C, 59.59; H, 2.95; N, 6.59%.

Acknowledgements

We wish to thank the Hellenic General Secretariat of Research and Technology for Financial Support with ΠΕΝΕΔ 99, ΕΔ 427.

Supplementary data

Supplementary data associated with this article can be found, in the online version, at doi:10.1016/j.tet.2006.01.064.

References and notes

1. For reviews see: (a) Collier, S. J.; Storr, R. C. *Prog. Heterocycl. Chem.* **1998**, *10*, 25–43. (b) Chou, T.-S. *Rev. Heteroat. Chem.* **1993**, *8*, 65–104. (c) Martin, N.; Seoane, C.; Hanack, M. *Org. Prep. Proced. Int.* **1991**, *23*, 239–272. (d) Segura, J. L.; Martin, N. *Chem. Rev.* **1999**, *99*, 3199–3246. (e) Pindur, U.; Enfanian-Abdoust, H. *Chem. Rev.* **1989**, *89*, 1681–1689.
2. Charlton, J. L.; Alauddin, M. M. *Tetrahedron* **1987**, *43*, 2873–2889.
3. Mann, J.; Piper, S. E.; Yeung, L. K. P. *J. Chem. Soc., Perkin Trans. 1* **1984**, 2081–2088.
4. Kametani, T.; Fukumoto, K. *Med. Res. Rev.* **1981**, *1*, 23–72.
5. Quinkert, G.; Stark, H. *Angew. Chem., Int. Ed. Engl.* **1983**, *22*, 637–655.
6. Kametani, T.; Nemoto, H. *Tetrahedron* **1981**, *37*, 3–16.
7. Nemoto, H.; Fukumoto, K. *Tetrahedron* **1998**, *54*, 5425–5464.
8. Valentin, C.; Freccero, M.; Sarzi-Amadè, M.; Zanaletti, R. *Tetrahedron* **2000**, *56*, 2547–2559.
9. Hwang, S. H.; Kurth, M. J. *Tetrahedron Lett.* **2002**, *43*, 53–56.
10. Mitkidou, S.; Stephanidou-Stephanatou, J.; Terzis, A.; Mentzafos, D. *Tetrahedron* **1992**, *48*, 6059–6068.
11. Joshi, K. C.; Jain, R.; Chand, P. *Heterocycles* **1985**, *23*, 957–996.
12. Mogilaiah, K.; Rao, R. B. *Indian J. Chem., Sect. B* **1998**, 894–898.
13. Marti, C.; Carreira, E. M. *Eur. J. Org. Chem.* **2003**, 2209–2219.
14. (a) Saroya, B.; Srinivasan, P. C. *Tetrahedron Lett.* **1984**, *25*, 5429–5430. (b) Pindur, U.; Gonzalez, E.; Mehrabani, F. *J. Chem. Soc., Perkin Trans. 1* **1997**, 1861–1867.
15. Vice, S. F.; Copeland, C. R.; Forsey, S. P.; Dmitrienko, G. I. *Tetrahedron Lett.* **1985**, *26*, 5253–5256.
16. Haber, M.; Pindur, U. *Tetrahedron* **1991**, *47*, 1925–1936.
17. Simulation program SpinWorks, version 2.2.0, available from ftp://davinci.chem.umanitoba.ca.
18. Jursic, B. S. *J. Heterocycl. Chem.* **1995**, *32*, 1445–1455.
19. Mitkidou, S.; Papadopoulos, S.; Stephanidou-Stephanatou, J. *J. Heterocycl. Chem.* **1991**, *28*, 1497–1499.
20. All calculations were carried out with MOPAC package version 6.3, *QCPE No. 455*, Indiana: Bloomington, IN.